Studies on Choline Graft Insulin Loadeded Chitosan Nanocomposite for Oral Delivery

R.Dhandayuthabani[1], M.Syed Muzammil[1], V.Sugantha Kumari[2], S.Khaleel Basha[3,*]

[1]*Department of Biochemistry, C. Abdul Hakeem College (Autonomous) Melvisharam 632 509, Ranipet District, TamilNadu, India.*

[2]*Department of Chemistry, Auxilium College, Vellore 632 006, India.*

[3,*]*Department of Chemistry and Biochemistry, C. Abdul Hakeem College (Autonomous) Melvisharam 632 509, Ranipet District, TamilNadu, India.*

Corresponding Author:-

Dr.S.Khaleel Basha

Assistant Professor, Department of Chemistry and Biochemistry, C. Abdul Hakeem College (Autonomous) Melvisharam 632 509, Ranipet District, TamilNadu, India.

Mail id:- khaleelnano@gmail.com

Abstract

This work sought to create insulin-loaded chitosan lipid hybrid nanocomposite (CLHNC) for oral administration. Insulin-loaded CLHNC were generated by ionic gelation-solvent evaporation process and their properties were characterized. Transmission electron microscopy (TEM) revealed that Insulin-loaded chitosan lipid hybrid nanocomposite (CLHNC) had a particle size of 200 nm with spherical shape and a zeta potential is 20-30 mV. The formulation components demonstrated the absence of interaction with the polymer, lipid and encapsulated drug, as confirmed by ATR/FTIR analysis. The Circular dichroism spectroscopy demonstrated insulin's structural stability under preparative stress, an *in vitro* leakage analysis revealed that the CLHNC maintained their integrity in simulated gastric fluid (SGF), and simulated intestinal fluid (SIF) juices. The CCK-8 test confirmed that the Insulin-loaded CLHC is safe for human colon adenocarcinoma (Caco-2) cells. A Caco-2 cell model was used to assess the apparent permeability (P_{app}) of insulin loaded CLHNC and unloaded CLHNC. The Confocal imaging was employed in the colon to authenticate enterocyte endocytosis. A synchronized delivery of insulin with improved mean residence time and half-life was supported by the pharmacokinetics investigation in male albino rats, and the nanocomposites (NCs) increased uptake and intracellular distribution in Caco-2 cells. These investigations point to the Insulin-loaded CLHNC a potentially useful nano carrier for insulin oral delivery due to its high stability, slow release, strong mucoadhesive properties, and other attributes.

Key words: *Diabetes mellitus, Oral drug delivery, Insulin, Nanochitosan synthesis Nanocomposite.*

1. Introduction

The metabolic condition known as diabetes mellitus (DM) is characterized by high blood sugar levels resulting from insufficiencies with either the secretion or the action of insulin [1]. According to World Health Organization predictions, DM is expected to be in seventh place among the leading causes of mortality worldwide by 2030 [2]. Insulin therapy is required to manage blood glucose levels and prolong survival in both type 1 and type 2 DM. In addition to pain, local tissue necrosis, infection, and nerve damage Apart from the associated risks of discomfort, infection, nerve damage, and local tissue necrosis [3], inadequate patient compliance has also been associated with frequent subcutaneous insulin injections. Furthermore, regular subcutaneous insulin injections have been linked to poor patient compliance also it is still believed that 5% of persons are needle phobic [4]. Oral insulin administration is therefore the recommended approach. It also conforms to the normal physiology of the insulin absorption pathway and is the most practical and non-invasive method, eliminating the danger of infection associated with injections [5]. It is also associated with important obstacles, including the gastrointestinal (GI) enzymes' breakdown of insulin and the tight junction, mucous lining, and epithelial mucosa's presence of an insulin absorption barrier [4-6]. In order to get beyond those challenges, we have chosen Chitosan is a naturally occurring cationic, mucoadhesive, mucopolysaccharide, and biocompatible polymer [7]. Because it's positively charged amino groups can create cross-links with negatively charged molecules in an acidic medium, Chitosan and its derivatives are widely employed [8]. mucoadhesive quality helps big molecular weight proteins bind more effectively and extends the amount of time the drug is present in the GI tract Besides serving as a regulated size of nanocarriers between 300 and 3000 nm [9]. Additionally, studies have demonstrated the potential use of Chitosan as a permeation enhancer for the absorption of hydrophilic drug compounds both *in vitro* and *in vivo* by mucosal surface and temporarily opening the epithelial tight junction between epithelial cells. It is assumed that this disruption of the epithelial tight junction is the cause of the effective oral drug delivery and good efficacy *in vivo* and *in vivo* [10]. Positively charged Chitosan and negatively charged lipid can interact by the use of ionic gelatins to create lipid chitosan hybrid nanocomposite, which have the benefits of both polymeric and liposomal drug delivery methods [11].

Protein encapsulation efficiency can be successfully increased by the solid lipid core-shell structure, and the outer lipid shell can shield the interior protein drug from GI proteases. In addition to offering several advantages over conventional formulations, such as good physical stability, spherical morphology, uniform size, positive zeta potentials, typical high cell penetration efficiency, core-shell pattern, and carbohydrates of generally recognized as safe (GRAS) status make the solid lipid delivery system all the more promising [12], the matrix of the solid lipid improves drug stability, avoiding proteolytic degradation after administration and releasing the drug in a controlled manner because multi-compartmental delivery systems can offer regulated and sustained release in a variety of applications, they have been used for medication delivery.

These systems comprise one or more compartments as well as protective outer shields. In particular, stimuli-responsive polymers can be sequentially encapsulated to incorporate both hydrophilic and hydrophobic medicinal compounds into these systems. For the oral delivery, several multi-compartmental systems have been created as a result [13]. The goal of this work was to combine the well-known biocompatibility advantages of the lipid matrix with the mucoadhesive properties and absorption-promoting effects of chitosan to develop a novel nanoparticulate carrier for insulin oral delivery. The innovative carrier consists of a lipid core that functions to maintain and control insulin release, and a mucoadhesive Chitosan layer that improves insulin retention during the course of the absorption window. Furthermore, we assessed insulin penetration using a variety of cell monolayer models and assessed the potential predictive power of these *in vitro* experiments for the degree of *in vivo* efficacy of the synthesized (NCs) in an animal model of diabetes.

2. Materials and Methods

2.1 Materials

All analytical-grade chemicals were used in our research study. Chitosan, Tripolyphosphate (TPP), solid Choline, span™ 80, Ethanol, were purchased by Sigma-Aldrich Mumbai. Insulin, Biphasic isophane, (40 I.U/ml), [(Human Mixtard, Monocomponent Biosynthetic *r*-DNA insulin obtained from Torrent Pharmaceuticals Ltd), (Novo Nordisk India Pvt Ltd)]. Caco-2 (human epithelial colorectal adenocarcinoma cell) was purchased from American Type Culture Collection (ATCC) (Rockville, MD, USA). For all the experiments, milli-Q water was used. All other chemicals used were of Good and Analytical grade.

2.2 Synthesis of Chitosan Nanoparticles (CNPs)

We prepared (CNPs) described previously as Solairaj D *et al.*, to prepare Chitosan 50 mg of Chitosan powder was dispersed in 50 mL deionized distilled water (1 mg/mL), under vigorous stirring, 1% acetic acid was added drop wise until the powder was completely dissolved [14]. The resulting Chitosan was subsequently diluted to various predetermined concentrations before being adjusted to pH 5 using 0.5 M NaOH. TPP was dissolved separately in deionized distilled water to a concentration of 1 mg/mL and adjusted to pH 2 with 0.1 M HCl. CNPs were formed by mixing 600 µL of Chitosan with increasing amounts of TPP solution (20-250 µL) and incubation for 5 minutes at room temperature. The NPs were then collected by centrifugation at 16,000×*g* for 90 minutes and the supernatant was discarded. The pellet was resuspended in 1 mL of deionized distilled water and 0.1 M acetic acid (50:1) and dispersed in solution by vortexing. The suspension was subjected to further centrifugation at 16,000×*g* for 45 minutes. The top 500 µL of the supernatant (containing the monodisperse CNPs) was collected and used for further experimentation. Alternatively, the CNPs-containing supernatant was freeze-dried to remove any excess acetic acid. The lyophilized CNPs powder was then weighed.

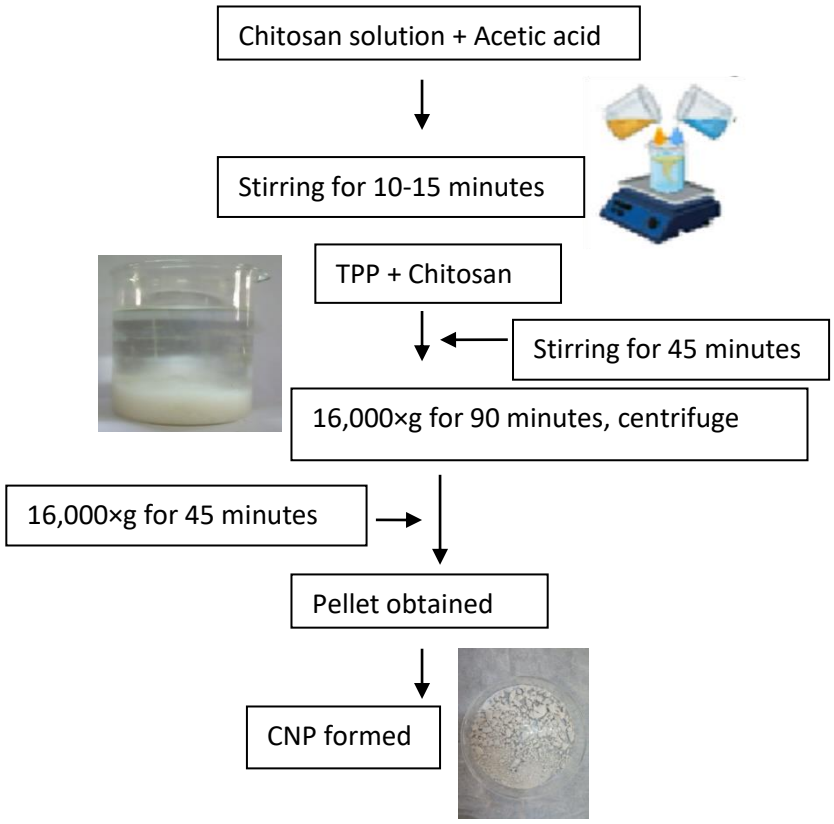

Figure 1. Synthesis of Nanochitosan (NC)

2.3 Preparation of drug loaded CLHNC

Fabricate of insulin loaded and unloaded CLHNC described previously by Solairaj D *et al.*, with slight modification. A simple process by emulsification / evaporation. In brief 50 mg of CNPs 800 µL of insulin solution, [150 mg insulin dispersed in 10 mL of PBS, 0.2 M at pH 7.4 (USP 34)], after gentle stirring for 30 minutes, 25 mg of the solid phospatidyl cholin was dissolved in ethanol (25 mg/ml) followed by addition of few ml of span-80 as surfactant after gentle stirring for 30 minutes at 800 rpm [15], in various concentration ratios (1:1, 1:3, 3:3) (Fig. 1). After 15 minutes of continuous spinning the insulin loaded CLHNC nanocomposites was formed. The optimum generated (NCs) ratio of 3:3 was chosen for further investigation.

3. Determination of Insulin Association efficiency (AE) and Loading capacity (LC)

An indirect method was used to calculate the AE by calculating the difference between the total amount utilized to produce the systems and the amount of insulin that remained in the aqueous phase following CLHNC isolation by filtration through a 0.2 µm filter, the amount of insulin entrapped into CLHNC was determined (Schleicher and Schuell, Germany). An HPLC-UV method that our group had previously developed and verified was used to determine the concentration of insulin in the filtrate solution [16]. The AE was calculated using the following formula.

$$\text{AE}\ (\%) = \frac{Total\ amount\ of\ Insulin - Amount\ of\ free\ Insulin\ in\ the\ Supernatant}{Total\ amount\ of\ Insulin\ added} \times 100$$

LC is the percentage of total CLHNC dry mass that represents the difference between the total amounts of insulin needed to generate the CLHNC and the quantity of unassociated insulin left over after particle separation. An aliquot weight of hydrated CLHNC that were obtained after isolation was freeze-dried to produce dry mass.

4. Determination of insulin

Insulin levels were determined using a reversed-phase HPLC ultraviolet (UV) technique [17]. The HPLC system (1100 series, Agilent Technologies, Santa Clara, CA, USA) consisted of a quaternary pump, a degasser, an auto-sampler, a column heater, and a tunable UV detector. A C18 column Zorbax, 5 m, 4.6 mm 150 mm, Agilent, and a C18 pre-column 2 mm 20 minutes, Alltech, were utilized for detection at 25°C. The mobile phase consisted of acetonitrile and 0.57% phosphoric acid solution adjusted to pH 2.25 with triethylamine in a volume ratio of 26:74. The detection wavelength was λmax 220 nm and the flow rate was set to 1.0 mL/min.

5. Characterization of both insulin loaded and unloaded CLHNC

5.1 Size and Surface morphology characterization

The average particle size and polydispersity index (PDI) of the produced NPs were estimated *via* laser dynamic light scattering. By diluting the NPs suspension to 1/50 v/v in HPLC water, the particle size investigation was carried out in triplicate. The particle size distribution of the NPs in a particular sample is shown by the PDI value. A higher PDI value denotes a distribution of NPs with a varied size range, which forms aggregates and may lead to low homogeneity and low stability of particle suspension [18]. The Malvern Zetasizer (Malvern, Worcestershire, UK) was used to assess the zeta potential of the NPs suspension after it had been diluted fifty times with HPLC water. The stability of the NPs in the suspension was assessed by measuring the zeta potential, which represents the surface charge on the particles.

5.2 Transmission Electron Microscopy (TEM) Analysis

Applying a transmission electron microscope (JEM-200 CX, JEOL, Tokyo, Japan), the surface morphology of the loaded and unloaded insulin CLHNC was examined. The loaded and unloaded insulin CLHNC sample was placed on a copper grid loadeded with carbon, vacuum-dried until it was totally dry, and then analyzed. After removing the extra sample from the grid, appropriate pictures were captured at various magnifications [19].

5.3 Attenuated Total Reflectance - Fourier Transform Infrared Spectroscopy (ATR-FTIR) Analysis

Employing the ATR-FTIR spectroscopy (TENSOR 27, Bruker, Germany) to identifying chemical compounds, molecular structures and surface properties of insulin loaded CLHNC and unloaded CLHNC were recorded. The lyophilized formulations KBr discs were made and examined between 400 and 4000 cm^{-1} in wavelength range [20].

5.4 Stability Study

The physical the stability of the CNP and CLHNC was assessed such as Hydrodynamic diameter, particle size distribution, and surface characteristics were tracked for 30 days at 4°C in suspension also previously indicated EE % and Recovery % studies over 30 days period. Physical permanence of CNPs and CLHNC was carried out in gastric conditions as follows. 5 mL of CLHNC nanocomposite suspension were incubated with an equal volume of simulated gastric fluid (0.32% w/v pepsin, 2 g of sodium chloride and 7 mL HCl dissolved in 1 L water and pH adjusted to 2.0 using 1M HCl) in a horizontal shaker for 2 hours at 37°C. The mixture was then shaken for an additional two hours at 37°C while simulated intestinal fluid (lipase 0.4 mg/mL, bile salts 0.7 mg/mL, pancreatin 0.5 mg/mL, and calcium chloride solution 750 mM at pH 7.0) was added. [21].

5.5 Conformational stability of Insulin

Making use of Circular Dichroism (CD) spectroscopy (Jasco J-810, Jasco Corp, Tokyo, Japan), the conformational stability of insulin was evaluated. By mixing 10 mL with a pH 1.0 hydrochloric acid solution and 4 mL of methanol, the loadeded CLHNC of 1 mL was eliminated. After centrifuging at 16,000 g for 10 minutes, insulin was separated from the supernatant. Subsequently, a Supelco ENVI-18 solid-phase extraction column (Sigma-Aldrich) was used to separate the insulin [22]. In summary, methanol was used to activate the ENVI-18 column before a solvent was added to balance it. Following that, a 1 mL supernatant mixture was plated. After removing contaminants with 3 mL of 40% aqueous methanol, the insulin was eluted using 30 mL of 60% aqueous methanol. Using a hydrochloric acid solution, the insulin concentration was increased to 30 μg/mL in order to conduct the CD test. Spectra were obtained at 20°C using a 0.5 nm step size, a maximum wavelength range of 200-300 nm, a band width of 3 nm, a 500 nm/minute scanning speed, and a 0.25-second reaction time. The secondary structure content was computed using the Jasco w32 secondary structure estimate software, version 1.0.

5.6 *In vitro* drug release

The rate and extent of insulin release as a model drug were investigated in mutually SIF, pH 6.8, duodenum pH and PBS, pH 7.4, colon pH to evaluate the feasibility of the recommended delivery system for peptide and protein oral delivery [23]. To test the *in vitro* release of insulin from CLHNC, 30 mg was combined with 500 mL of SIF solution and shaken at 50 rpm. The temperature remained at 37°C±5°C. To reach the sink condition, the releasing medium was designed to be quite large. At specified intervals, 1 mL aliquots were drawn and replaced with preheated blank media. For 20 minutes, the samples were centrifuged at 14,000 rpm. Instead of adding blank medium following aliquot removed, the supernatant was analyzed for insulin concentration, and the sediment was dispersed in 1 mL blank media earlier than reintroducing it into the release medium because the insulin release from the CLHNC polymeric mesh did not finish within the first few hours, the remaining insulin in the withdrawn CLHNC was also released. The insulin concentration in the supernatant was determined using a previously described HPLC procedure. To further recognize the process of peptide release from the nanoparticulate drug delivery device, *in-vitro* insulin release data was fitted to the Ritger-Peppas equation.

$$\frac{M_t}{M_\infty} = Kt^n$$

M_t and M_∞ denote cumulative insulin release at time (*t*) and infinite time, respectively. *K* is a constant related to the device's structural and geometric properties, while '*n*' is an exponent reflecting the diffusion mechanism. The number of calculated values for '*n*' was used to find the release mechanism. If n = 0.45, the release mechanism is Fickian/case I diffusion, 0.45 < n < 0.89, non-Fickian/anomalous transport, and n = 0.89, diffusion and zero-order (case II) transport.

5.7 Transepithelial electrical resistance (TEER) and insulin transport studies

The Caco-2 cell lines were cultured in transmembrane inserts with a cell density of 5×10^5 cells/well and a pore size of 0.4 μm (Millipore). The TEER of the cell monolayer was measured at predefined intervals at 37°C using 10 mg/mL/well concentrations of the insulin loaded CLHNC and without insulin loaded [24], CLHNC as a blank, aspart insulin, a new and short-acting analogue of human insulin, was also loaded in either the plain insulin loaded CLHNC and without insulin load CLHNC as a blank with the same concentration, aspart insulin's monomeric structure and linear shape in aqueous media provide it greater ability to cross the lumen epithelium. We examined both human insulin and aspart insulin under the identical conditions and compared the outcomes in order to assess this potential and determine whether this CLHNC system performs better with insulin. As a control, a simple solution containing aspart insulin and human insulin was administered to the donor chamber of the cell layer. For the purpose of insulin transport investigations, fresh medium containing insulin-NC and blank (10 mg/well) was added to the donor chamber medium. Throughout the course of four hours, aliquots were obtained from the receiver chamber at prearranged intervals, and the samples' insulin content was examined. Every instance was examined three times, and the mean values were shared. The formula P_{app} = (dQ/dt) /A is as follows. Insulin's apparent permeability coefficient ($P_{app)}$ was computed using C_0. The permeability rate, dQ/dt, the filter membrane's surface area, and the starting insulin concentration in the apical chamber, C_0, are all represented in this equation.

$$Papp = \frac{\frac{dQ}{dt}}{A \times C_0}$$

5.8 *In vitro* cytotoxicity of CLHNC

The Caco-2 cells proliferate in environments with elevated glucose levels. 10% foetal bovine serum, 1% v/v non-essential amino acids, 50 U/mL penicillin, and 50 μg/mL streptomycin are included in Dulbecco's modified Eagle medium. For 21 days, Caco-2 cells were grown in monolayer culture [24]. For the first fifteen days, the culture media was changed every two days, and for the final week, it was changed daily. The cells were cultured at 37°C in 5% CO_2. The MTT assay was performed to evaluate the cytotoxicity of an insulin-loaded CLHNC on Caco-2 cells over the course of 24 hours. In order to enable confocal microscopy imaging, Caco-2 cells ($1x10^5$ cells/well) were cultivated in 6-well plates for duration of 24 hours. Subsequently, sterile glass cover slips were placed over the wells. The cells were treated with insulin-FITC and insulin-FITC loaded CLHNC-insulin at 10 μg/mL doses at staggered time intervals. Before being observed under a confocal microscope (CLSM, Carl

Zeiss Microscopy GmbH, Germany), cell monolayers were thoroughly cleaned with PBS pH 7.4. Caco-2 cells that were planted one at a time were exposed. A 1 mM folic acid solution was added to the cells beforehand to prevent receptor-mediated endocytosis. After that, the cells were treated for four hours at 37°C with an insulin-loaded CLHNC containing 10 µg/mL insulin. Cold PBS was used to wash the cells three times before they were lysed with 0.1% Triton X-100. The manufacturer-recommended ELISA kit was used as a control to measure intracellular insulin absorption in the absence of inhibitors.

5.9 *In vivo* pharmacokinetics

In vivo investigations on insulin-loaded CLHNC in male albino wistar rats with diabetes. The 200-250 g male albino wistar rats were utilized in all studies, and their living quarters were maintained at a consistent temperature of 22± 2°C and relative humidity of 45-65%. The rats were given tap water on a constant basis along with regular diet feed (Mucedola Top Certificate, Italy). Standard 12 hour on/12 hours off lighting cycles were in place. A single intraperitoneal injection of streptozotocin (50 mg/mL in citrate buffer, pH 4.5) at a dose of 50 mg/kg body weight was used to cause diabetes in rats. The Rats with fasting blood glucose levels more than 250 mg/dL were employed for the investigations after two weeks. These rats were given free access to water without restriction; they were fasted for 12 hours prior to the experiment and for 24 hours during it. Rats were given a gavage needle injection of CNPs-loaded lipid and CNPs dispersions (1.0 mL PBS) at an insulin dose of 25 IU/kg, which was determined by the total insulin content of the CNPs. Similarly sized quantities of insulin oral solution (25 IU/kg in PBS) were given to control rats. The investigation also included a control group that received subcutaneous insulin treatment (2.5 UI/kg).Following a needle puncture, blood samples were taken from the tip of the tail vein. At regular intervals both before and after injection, a 0.1 mL aliquot was taken. The determination of the pharmacological availability (P_A) of peroral insulin loaded CLHNC was conducted by administering a control solution subcutaneously to diabetic rats at a dose of 2.5 IU of insulin/kg, with 100 % availability. The trapezoidal approach was used to calculate the area above the curve (AAC) below the 100% cut-off line when plasma glucose levels were plotted against time [25].

Oral P_A ¼ AAC = oral dosage AAC S_c = 100 dosage Sc The blood glucose level was measured as a percentage of the baseline plasma glucose level using the Medisense Precision Xceed Kit (Abbot, Portugal), with a range of 10-600 mg/dL. The findings are displayed as the average of data (±SEM) from a minimum of six animals. For every rat, the cumulative hypoglycemia effect and the cumulative insulin supplied to plasma were computed, and treatment differences were assessed using a one-way analysis of variance. A post hoc test (S-N-K) was used to compare the differences between the groups if the group by each time interaction was significantly different ($p<0.05$). The SPSS software program was used for all statistical analyses (SPSS for Windows 14.0, SPSS, Chicago, USA).

6. Statistical Data Analysis

The mean and standard deviation of the results were displayed. Groups were compared using a one-way analysis of variance (ANOVA) (SPSS 16.0, IBM Corp, Amonk, NY). If a difference had a *P*-value of less than 0.05, it was considered statistically significant.

7. Results and Discussions

7.1 Particle size and surface charge

The loading and release of the drug from the nanocomposite formulation are influenced by the size and polydispersity index [26]. All formulations' particle sizes and zeta potentials are displayed in (Table 1). All of the developed formulations had particle sizes ranging from 200 nm, which is appropriate for passively diabetes mellitus, because of the electrostatic interaction between chitosan and lipid, the surface charge at the 3:3 ratio of lipid-chitosan is remained positive. Chitosan cationic charge is predominant. Nevertheless the zeta potential value changed from positive to negative as the lipid content ratio. Interplay of negative and positive charges at the right concentration led to the observation of a mono dispersity and improved stability profile at a ratio of 3:3.

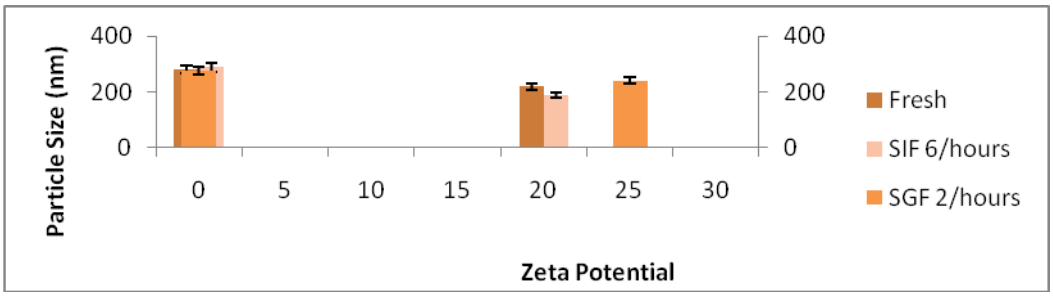

Graph 1. Effect on Particle Size and Zeta Potential

Table: 1

Effect of the lipid and nanochitosan ratio on particle size (z-average), surface, charge, AE and loading capacity

lipid- NC Ratio	Particle size (nm)	PDI	Zeta potential (Mv)	AE (%)	LC (%)
3:3	200+- 0.34	37.1+-1.3	20-30 mV.	83.2+-1.2	1.69+-0.5

Results - indicate average Mean±SD n=3, AE - Association efficiency, DL - Drug Loading.

7.2 AE and LC

By using an indirect method, the amount of drug entrapment in the CLHNC was estimated while maintaining a constant drug concentration; parameters were assessed at various lipid and chitosan concentrations. Over 70% of the formulations exhibited association efficiency. The greatest association efficiency. was demonstrated by CLHNC at a ratio of 3:3 (89.2%) because the hybrid NPs have a lipid layer, they showed noticeably better drug loading capacity and association efficiency. than polymeric NPs. Drug association was enhanced by the lipid coat that covered the polymer's exterior, providing structural stability and preventing hydrophilic medicines from leaking [27].

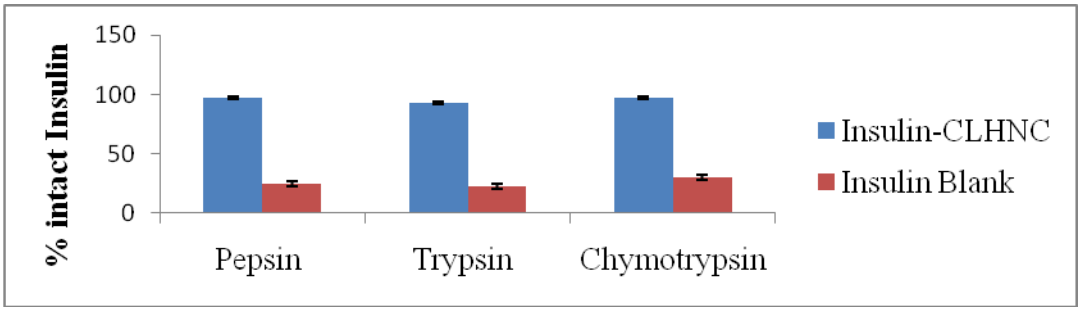

Graph 2. Effect on Association efficiency

7.3 Morphology of the insulin loaded and unloaded CLHNC

Transmission electron microscopy was used to examine the morphology of the CLHNC with and without insulin added [28]. The TEM pictures revealed the 200 nm spherical NPs with the lipid and polymer lipoplex structure entangled with one another due to positive and negative charge in the hybrid NPs (Fig. 2a,b). The pictures showed a lipoplex shape with some lipid coating, which stopped water and drug from penetrating the system and causing diffusion. The chitosan-lipid shell gives the system its long-circulating properties.

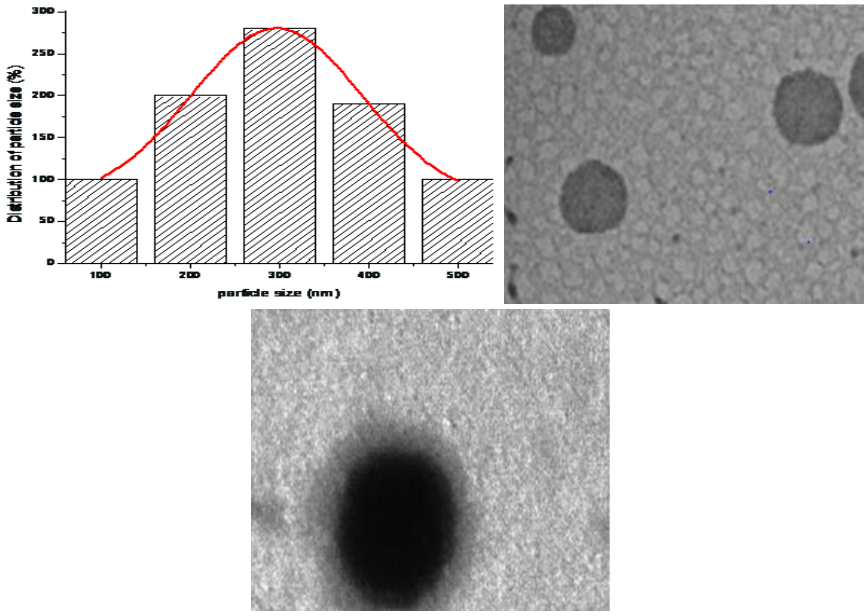

Figure 2 a. Histogram of nanocompoite. 2.b.TEM of Drug loaded and unloaded CLHNC

7.4 ATR-FTIR SPECTROSCOPY

ATR-FTIR analysis of the interactions between the polysaccharide and the lipid has revealed the structure of these CLHNC. Figure 3 reproduces the ATR-FTIR spectra of nanoparticles and of the components choline and chitosan. The characteristic absorption bands of choline, the primary constituent of the nanocomposite are visible in the infrared spectra of the nanoparticles. In actuality the chitosan characteristic band at 1590 cm−1, which corresponds to the NH2 scissoring vibration of the main amino group, was absent from the nanoparticle spectra. This occurrence was most likely caused by the ionic contact between the phosphate groups of choline and the ammonia groups of chitosan that formed in an acidic solution.

Conversely, the chitosan amino group's usual absorption peak remained visible at 1660 cm−1. Additionally, the stretching of the fatty acid carbonyl groups resulted in a decrease in the intensity of the absorption band at 1738 cm−1 in the nanoparticle spectrum when compared to choline alone. The phosphate group absorption band shifted from 1236 cm−1 in the lecithin to 1217 cm−1 in the nanoparticle sample. This suggested that there had been ionic interactions between the amino groups of chitosan and the groups of phosphate of choline. A polysaccharide coating has been shown to dramatically lower the mean square fluctuations in polipeptides, resulting in quasi-harmonic behavior that is nearly room temperature [20]
The ATR -FTIR analysis-based formulation components' chemical compatibility has been used to elaborate on the success of the proposed CLHNC It was discovered that CLHNC's physicochemical characteristics—such as size, morphology, polydispersity, drug entrapment, and drug content were ideal for oral drug administration.

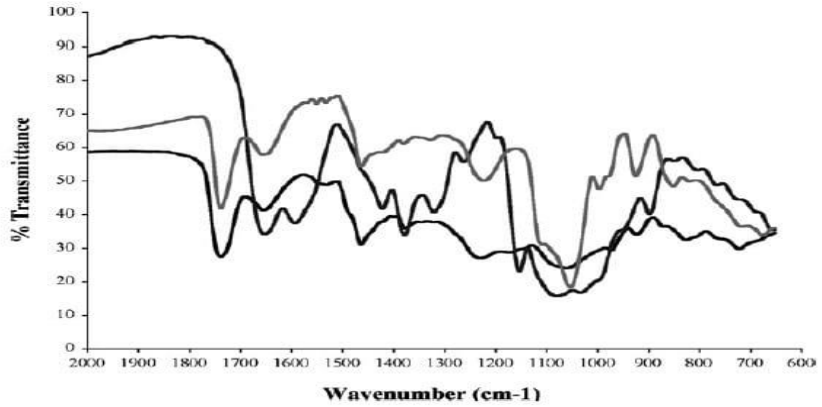

Figure 3. ATR -FTIR Spectrum of (a) CLHNC (b) NanoChitosan. (c) Choline

7.5 Physical stability

The primary determinants of CLHNC bioavailability are particle size, dispersion, and physical stability. We investigated the effects of insulin peptide concentration, sonication, homogenization, lipid-to-polysaccharide ratio, pH, and polydispersity index (PDI) on the particle size, physical stability, and PI of CLHNC.

7.6 Conformational stability of Insulin

Physical stability, in addition to particle size and dispersion, is widely recognized as a critical factor in regulating the bioavailability of CLHNC. In this study, we looked at how the particle size, physical stability, and PDI of CLHNC were affected by pH, polydispersity index (PDI), calcium binding efficacy, and polysaccharide to lipid ratio. It is possible to denature proteins and peptides through mechanical manipulation, exposure to organic solvents, and high temperatures. For this reason, appropriate therapeutic efficacy is crucial. Therefore, when altering peptides or proteins, conformational stability needs to be considered. Circular dichroism spectroscopy is a powerful tool for studying protein and peptide secondary structures, like the α-helix and β-fold, which can show the potency of insulin. Circular dichroism is Figure 4 displays the spectroscopic spectra of insulin secondary structures.

The spectra of CLHNC that was loaded and unloaded with insulin had the same peak valley at around 206-208 nm and shoulder at approximately 222-226 nm as the insulin solution. The secondary structures of insulin, which comprised 21%–22% α-helix and 27%–29% β-folds, were consistent among samples. This secondary structural analysis demonstrates that the conformational shape of insulin did not alter throughout the synthesis of CLHNC with and without presence of insulin.[22[

7.7 *In vitro* Drug Release

Graph 3 shows the *in-vitro* release curve of model peptide insulin from an optimized CLHNC delivery device loaded with the embedded peptide during a post-loading operation (29)]. The release profile was assessed at SIF pH 6.8, SGF pH 1.2, and phosphate-buffered saline pH 7.4. Both media demonstrated a spike of insulin release during the first 30 minutes, which thereafter decreased but remained constant over the next 24 hours. During the burst release phase, almost 33%±6% of total insulin is released at pH 7.4, 20%±2.1% at pH 6.8, and 22%±2.3% at pH 1.2.

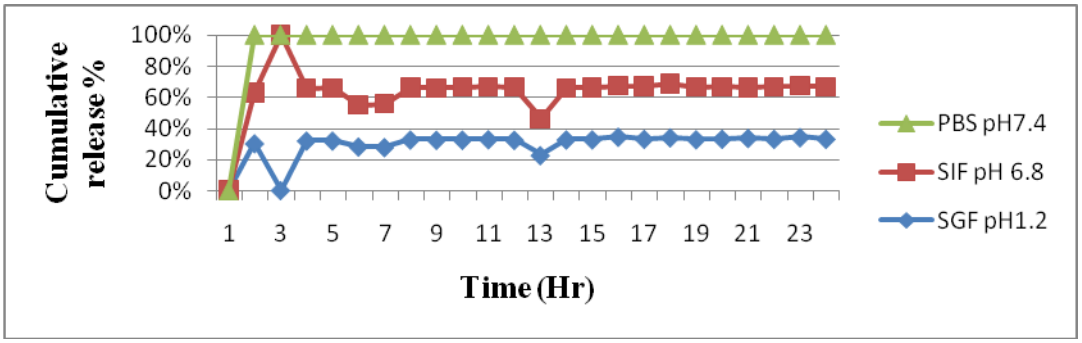

Graph 3. CLHNC-insulin Release profile from PBS pH 7.4, SIF pH 6.8, and SGF pH 1.2

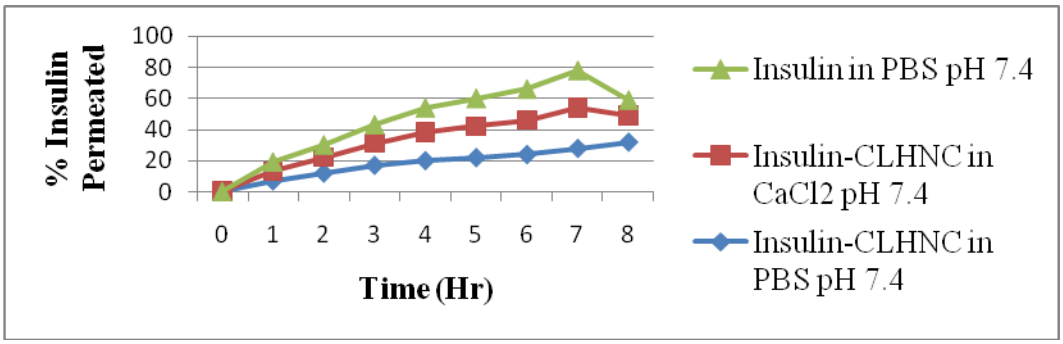

Graph 4. Insulin permeability in the rat gut and the influence of several stomach enzymes

We discovered through optimization testing that CLHNC with specific polysaccharide and lipid contents obtained the maximum loading efficiency, release behavior, and total release extent. In phosphate-buffered saline pH 7.4, 86% of the implanted insulin had been released after a full day, suggesting that insulin release from the optimized CLHNC was nearly complete. In SIF pH 6.8, 1.2, and phosphate-buffered media, the rates of insulin release for both burst and total were reduced (20%±2.1% for burst and 78%±6.5% for total, respectively).

The protonation of many key carboxy groups in NC at pH 6.8 may still be present, keeping them cationic and attracting negatively charged insulin while delaying release. At pH 7.4, this formulation demonstrated an incredibly powerful burst and complete release .The impact of different stomach enzymes on the rat gut's ex-vivo insulin permeability is depicted in Graph 4. The polysaccharide in this formulation is water soluble at all pH values due to its amphiphilic characteristics. In addition to being normally soluble, the polysaccharide may not have been able to bind to and hold negatively charged insulin at this pH due to the loss of its cationic charge. For peptides with short half-lives, like insulin, this quick peptide release from the CLHNC polymeric mesh is advantageous since it keeps the therapeutic benefits of the delivery mechanism intact.

7.8 Transepithelial electrical resistance (TEER) and insulin transport studies

Transmembrane inserts with a pore size of 0.4 μm (Millipore) and a cell density of 5×105 per well were used to cultivate Caco-2 cell lines. TEER studies were conducted using a previously published approach. At specified intervals and at 37°C, the TEER of the cell monolayer was measured using either plain CLHNC or CLHNC-insulin loaded at a concentration of 10 mg/mL/well. aspart insulin, a brand-new, short-acting human insulin analogue, was also loaded into plain CLHNC or CLHNC -insulin loaded at the same quantity, per certain investigations [8]. Because aspart insulin is monomeric and has a linear shape in an aqueous media, it can pass through the lumen epithelium more easily.

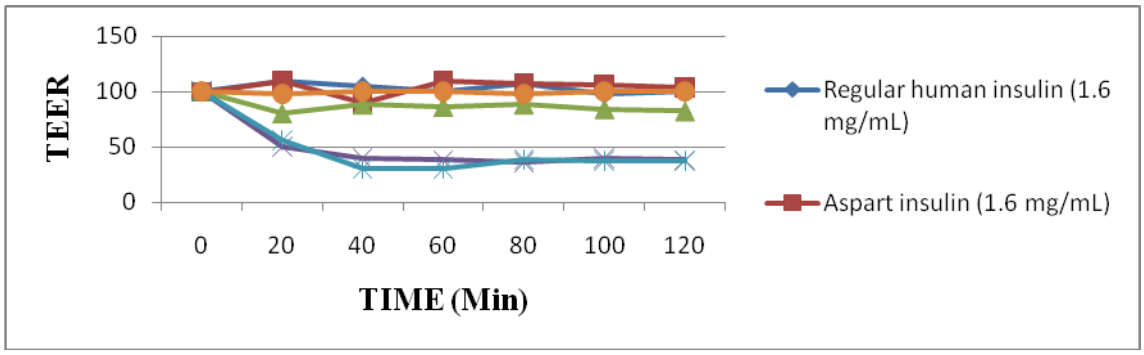

Graph 5. Outcome of diverse formulations on TEER

To determine if our CLHNC method performed better than aspart insulin, we compared the same conditions to human insulin and aspart insulin (Alpha Diagnostic International). In the donor chamber of the cell layer, a simple solution containing both human and aspart insulin was injected as a control. The donor chamber medium was swapped out for fresh media containing either plain CLHNC or CLHNC -insulin loaded (10 mg/well) for the purpose of insulin transport investigations. Over the course of four hours, aliquots from the receiver chamber were taken at predetermined intervals, and the insulin content was determined using a specialized ELISA kit that was sensitive to aspart insulin as well as regular human insulin. For each instance that was evaluated in triplicate, the average findings were shown. The following formula was used to get insulin's apparent permeability coefficient (Papp). The permeability rate is denoted by dQ/dt in this equation, the surface area of the filter membrane is represented by A, and the initial insulin concentration in the apical chamber is represented by C_0.

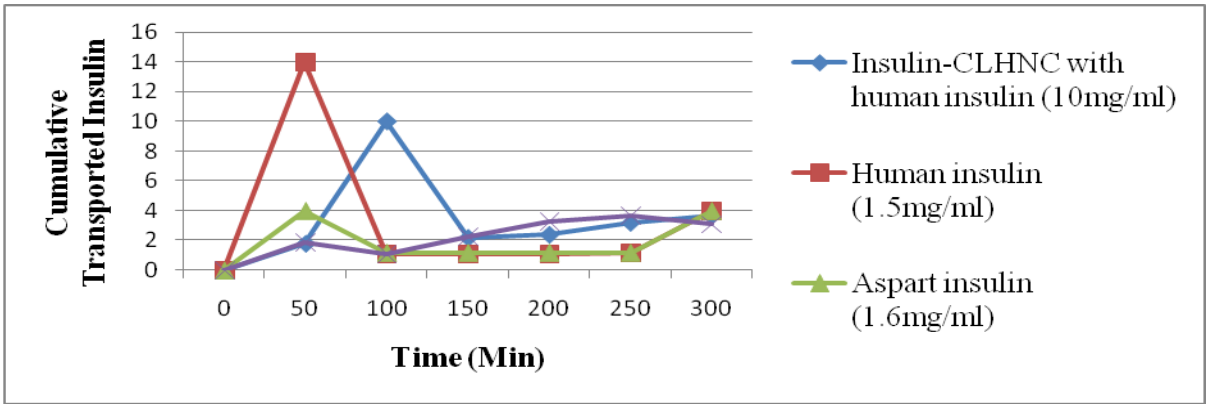

Graph 6. Collective transported formulation of insulin

7.9 *In vitro* cytotoxicity of CLHNC

Cell viability was over 90% at dosages comparable to 10 μg/mL insulin (Fig. 4). Cell viability drastically decreased ($p<0.05$) when insulin CLHNC concentrations increased, most likely due to an increase in NC content. The ensuing mild positive charge value of CLHNC generally increases its safety. Consequently, an NC-insulin containing fat and insulin equivalent to 10 μg/mL was employed in subsequent studies.

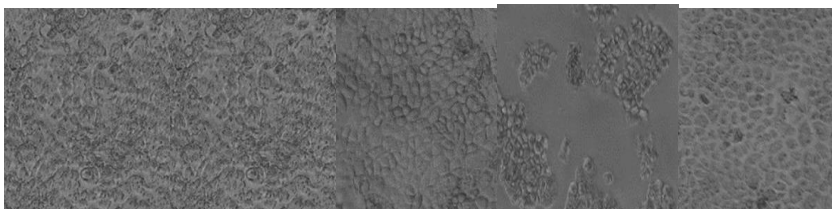

Figure 4. Images of Light microscope as Caco-2 exposure to (a) insulin-FITC for 5 hr ,CLHNC-insulin for 1,2,3,4 and 5 hours

7.10 *In-vitro* Caco-2 cellular uptake

Caco-2 cells did not produce any fluorescence after being incubated with insulin-FITC for 5 hours (Figure 5) The high molecular weight of insulin prevents internalization by cells. On the other hand, a lot of green fluorescent spherical particles were visible in the CLSM micrographs of a CLHNC-insulin, which suggests that the insulin has been internalized by the cells. Moreover, the fluorescent dye's intensity increases with incubation time.

7.11 Tracking the insulin-CLHNC cellular uptake pathway

Figure 4 shows the outcomes of this experiment. In Caco-2 cells, CLHNC significantly decreased insulin absorption ($p<0.05$), suggesting that CLHNC-insulin can improve insulin internalization. To identify the mechanism of CLHNC uptake, Caco-2 cells were pre-treated with a variety of chemical agents. The results showed that clathrin-mediated endocytosis, caveolae-mediated endocytosis, macropinocytosis, and microtubular-mediated endocytosis were the responses to chlorpromazine, nystatin, amiloride, and colchicine, respectively. Graph 6 shows that all inhibitors, with the exception of chlorpromazine, significantly decreased the cellular internalization of insulin nanoparticles ($p>0.05$). This indicates that clathrin-mediated endocytosis is not a transporter mechanism for insulin-CLHNC.

Conversely, nystatin is a cholesterol-binding medication that prevents caveolae-mediated endocytosis by sag formation [33]. Previous research has demonstrated that in order to deliver nanocargo to caveosomes and prevent the degradative lysosomal pathway, caveolae-mediated endocytosis entails detaching caveolae from the plasma membrane. Amiloride also prevents the plasma membrane's essential Na+/H+ exchange, which is a phase that is required for macropinocytosis to occur. Colchicine decreases microtubule-mediated endocytosis by irreversibly binding to tubulin and preventing microtubule polymerization. Because the cell membrane is negatively charged and contains heparan sulphate proteoglycans, microtubules generally form a cytoplasmic network that takes part in endocytic vesicle trafficking. Enzymes called heparinases hydrolyze certain proteoglycans that are present on cell membranes, reducing their harmful effects. When Caco-2 cells were pre-treated with enzymes, the less negative cell membrane and the cationic nanoparticles had less electrostatic interaction, which led to an 80% reduction in insulin cellular internalization. Lastly, the particles are transported by non-destructive caveolae-mediated endocytosis, which targets Vitamin B12 receptors.

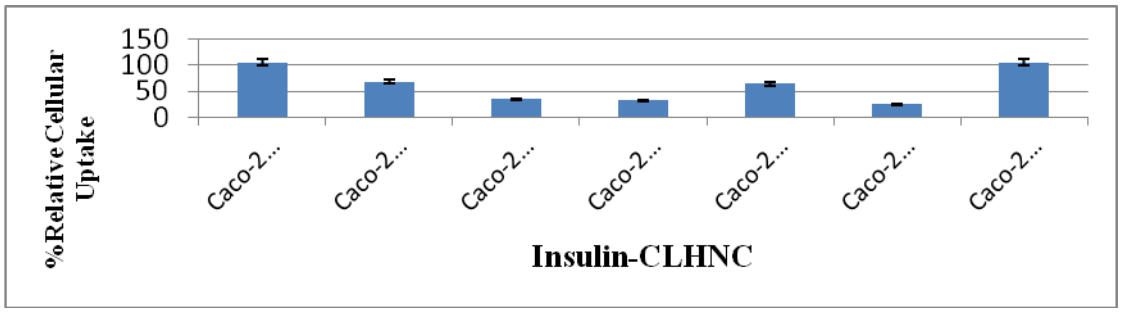

Graph 7. The effect of various endocytosis inhibitors on Caco-2 cellular insulin uptake after incubation with a NC-I.

7.12 *In vivo* Pharmacokinetics

In order to ascertain the impact of insulin-loaded CLHNC, the drug was analyzed by administering an identical dosage to two cohorts of six male albino rats. In order to assess the pharmacokinetics parameters, a concentration versus time relationship graph was created (Graph. 5). According to this research, phospholipid and polymer together have the potential to significantly affect pharmacokinetic characteristics and act as a vehicle for regulated administration [32]. For the drug solution group, it took 1±0.05 hours to attain maximal concentration, while for the CLHNC formulation group, it took 6±0.15 hours. Maximum blood concentration was 1.01 mg/mL as opposed to 4.07 mg/mL in the group receiving the drug solution. In order to extend exposure and lessen the negative effects of chemotherapy medications, a lower peak concentration is thought to be beneficial. The insulin-loaded CLHNC formulation had a half-life of 14.0±0.4 hours, which was significantly longer than the drug solution group's half-life of 1.25±0.04 hours. This suggests a regulated, sustained release of the drug As the mean residence time (MRT) in the lipid-polymer hybrid formulation was 20.8±0.3 hours as opposed to 6.0±0.5 hours in the insulin drug solution, this suggests that the formulation offers a regulated release of insulin.

It has been noted that the lipid layer enhances absorption and shields drugs from protein binding. Nakano *et al.*, (1997) reported a comparable rise in MRT for an insulin formulation. In comparison to the drug solution, which had an AUC of 18.4±0.5 mg h/mL, the CLHNC formulation had an AUC of 9.83±0.3 mg h/mL. Similarly, the CLHNC formulation group shows a 4.6-fold increase in volume of distribution of insulin as compared to the insulin solution. Kai *et al.*, also showed a 4.2-fold increase in volume of distribution of insulin. Overall, the CLHNC parameters significantly improved the insulin pharmacokinetics parameters.

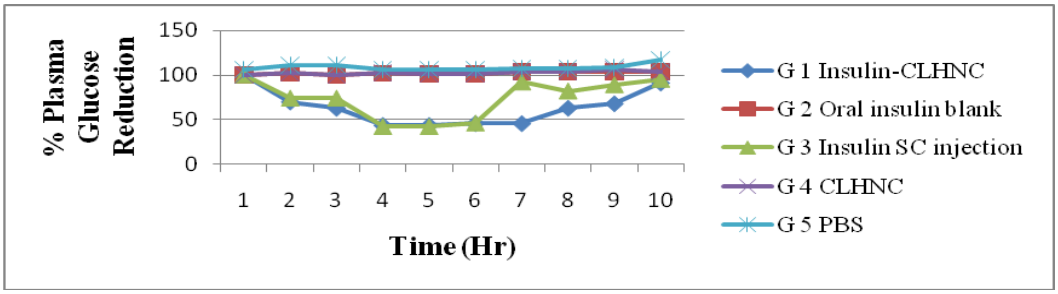

Graph. 8. (%) drop in plasma glucose after treatment

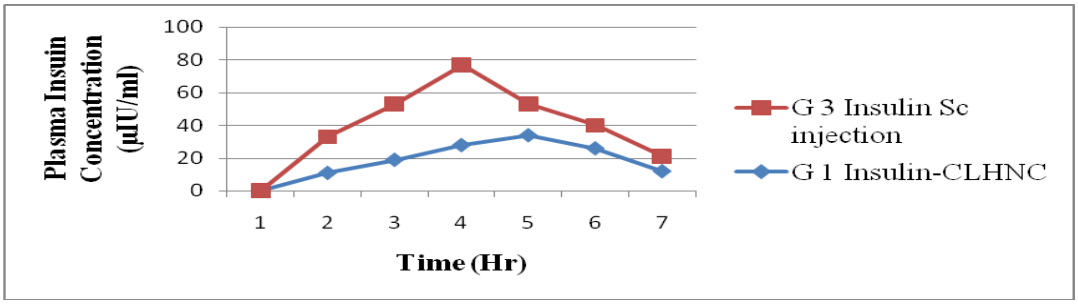

Graph. 9. Plasma insulin concentrations after oral I-CLHNC and Sc injection

Table 2. Pharmacodynamics of oral CLHNC - Sc insulin delivery

Groups	Initial plasma glucose conc. mg/dL)±SE	Pharmacodynamics parameters ± SE			
		Cmin (mg/dL)	Tmin (hr)	AUEC0-∞ (mg h/dL)	Total decrease in p.glu (%)
Group 1 received oral NC-Insulin	* 259.83±5.32	118.66±8.38	6hr	1690.11±3.47	32.41±2.74
Group 3 received insulin SC injection**	255.83±4.98	91.33±4.24	4hr	1814.59±3.24	27.45±2.55

Table 3. Pharmacokinetics - after oral CLHNC treatment, Sc insulin

Groups	Pharmacodynamics parameters ± SE				
	Cmax (µIU/mL)	Tmax (h)	AUC0-∞ (µIU h/mL)	MRT (h)	Relative bioavailability
Group 1 oral NC-Insulin	* 31.04±1.11	6hr	502.67±15.74	13.28±1.02	17.04%±1.34
Group 3 received insulin Sc injection	** 43.91±2.06	4hr	294.61±19.67	8.10±0.32	100

Results are the mean of six replicate±SE. *Insulin dose 50 IU/Kg. **Insulin dose 5 IU/Kg.

7.13 Intestinal uptake

Histocompatibility was demonstrated by the rat intestinal mucosa, which did not exhibit any histological changes after oral administration of CLHNC-insulin. Following oral administration of the insulin-FITC solution, no fluorescence was observed in any area of the colon (Fig. 4a,b,c). This may be because insulin cannot pass through intestinal walls and breaks down quickly in the gastrointestinal system. On the other hand, fluorescence was seen all over the digestive system. As previously shown, CLHNC-insulin may shield insulin from enzymatic degradation in the gastrointestinal tract. Remarkably, the CLHNC was discovered on the mucosal surface, deep within the muscular areas and submucosa. The negatively charged cell membrane and the positively charged CLHNC interacted electrostatically to keep the CLHNC on the mucosa. In the Peyer's patches, a CLHNC -insulinn was also discovered. Previous studies found that adsorptive endocytosis was mostly responsible for the internalization of CLHNC in Peyer's patches. The ability of CLHNC to enter the intestinal wall is made possible by its superior qualities, which include mucoadhesion and penetration augmentation through the opening of cellular tight junctions [12]. These results showed that both transcellular and receptor-mediated endocytosis were part of the paracellular pathway. These results are in agreement with the mechanism of cellular absorption.

8. Conclusion

Synthetic chitosan lipid hybrid nanocomposite (CLHNC) loaded with insulin were adequately constructed and investigated for multiple physicochemical factors, such as particle size, drug loading, entrapment effectiveness, excipient compatibility, and in vitro drug release profile. The optimal formulation exhibited monodispersity, compact size, and a regulated release profile with an appropriate lipid and chitosan combination. A decrease in the lipid concentration has an impact on the drug's further release. Both polymers and lipids contributed to the drug's release rate. The polymer matrix and a lipid layer that stops drug leakage both regulate how much of the drug is released. There was no burst release of insulin because it was contained between the inner polymer layer and the outer lipid coating. Cell viability tests confirmed the cytotoxic effect Caco-2 cells underwent during a 24-hour incubation period. Research on the absorption of cells showed that CLHNC was more cellular absorbed. Studies on the in vivo pharmacokinetics of rats demonstrated a regulated release pattern. Toxicity studies in rats provided safety profile of the CLHNC.

According to these studies, the insulin-loaded CLHNC has strong mucoadhesive qualities, excellent stability, enhanced bioavailability, slow release, and other qualities that make it a viable alternative and possibly helpful nanocarrier for oral insulin delivery in the treatment of diabetes mellitus.

References

1.Sun, H.; Saeedi, P.; *et al.*, D. J. IDF Diabetes Atlas: Global, Regional and Country-Level Diabetes Prevalence Estimates for 2021 and Projections for 2045. Diabetes Res. Clin. Pract. 2022, 183, 109-119.

2. Mulka, A.; Lewis, B. E.; Mao, L.; Sharafieh, R.; Kesserwan, S.; Wu, R.; Kreutzer, D. L.; Klueh, U. Phenolic Preservative Removal from Commercial Insulin Formulations Reduces Tissue Inflammation While Maintaining Euglycemia. ACS Pharmacol. Transl. Sci. 2021, 4 (3), 1161-1174.

3. Baruah, P.; Das, A.; Paul, D.; Chakrabarty, S.; Aguan, K.; Mitra, S. Sulfonylurea Class of Antidiabetic Drugs Inhibit Acetylcholinesterase Activity: Unexplored Auxiliary Pharmacological Benefit toward Alzheimer's Disease. ACS Pharmacol. Transl. Sci. 2021, 4 (1), 193-205.

4. Danta, C. C. Dipeptidyl Peptidase-4: A Potential Therapeutic Target in Diabetic Kidney Disease with SARS-CoV-2 Infection. ACS Pharmacol. Transl. Sci. 2020, 3 (5), 1020-1022.

5.Syed Muzammil,M; Dhandayuthabani, R; Sugantha Kumari, V; Khaleel, Basha S; Probing insulin bioactivity in oral nanoemulsion produced by emulsification assisted electrostatic self assembly cross linking method : an peer-revi acad journ 0477 volume 23 : issue 02 (Feb) - 2024

6.Syed Muzammil,M; Dhandayuthabani, R; Sugantha Kumari, V; Khaleel, Basha S; Development of pH sensitive nanopectin/insulin based nanoemulsion for oral insulin drug delivery: an peer-revi acad journ volume 23 : issue 02 (Feb) – 2024

7.Khaleel Basha, S; Syed Muzammil, M; Dhandayuthabani, R; Sugantha Kumari ,v ; Polysaccharides as excipient in drug delivery system Journal of Materials Today: Proceedings, 2020.04.046.

8. Lewis GF, Brubaker PL. The discovery of insulin revisited: lessons for the modern era. J Clin Invest 2021, 131(1).

9. Shetty SS, Halagali P, Johnson AP, Spandana KA, Gangadharappa HV. Oral insulin delivery: barriers, strategies, and formulation approaches: a comprehensive review. Int J Biol Macromol 2023, 242(3):125114.

10. Benyettou F, Kaddour N, Prakasam T, Das G, Sharma SK, Saet al Thomas. *In-vivo* oral insulin delivery via covalent organic frameworks. Chem Sci 2021,12(17): 6037-47.

11.Iyer G, Dyawanapelly S, Jain R, Dandekar P. An overview of oral insulin delivery strategies (OIDS). Int J Biol Macromol 2022.

12. Bashyal S, Seo JE, Keum T, Noh G, Lamichhane S, Lee S. Development, characterization, and ex vivo assessment of elastic liposomes for enhancing the buccal delivery of insulin. Pharmaceutics 2021,13(4):565.
13.Guo Y, Yang Y, Xu Y, Meng Y, Ye J, Xia X, *et al.,* Deformable nanovesicle-loaded gel for buccal insulin delivery. Pharmaceutics 2022,14(11):2262.
14. Diab M, Sallam AS, Hamdan I, Mansour R, Hussain R, Siligardi G, *et al.,* Characterization of insulin mucoadhesive buccal films: spectroscopic analysis and *in vivo* evaluation. Symmetry 2021,13(1):88.
15. Li M, Sun Y, Ma C, Hua Y, Zhang L, Shen J. Design and investigation of penetrating mechanism of octaarginine-modified alginate nanoparticles for improving intestinal insulin delivery. J Pharmaceut Sci 2021,110(1):268-79.
16. Bialik M, Kuras M, Sobczak M, Oledzka E. Achievements in thermosensitive gelling systems for rectal administration. Int J Mol Sci 2021,2217.
17.Li J, Zhang Y, Yu M, Wang A, Qiu Y, Fan W, *et al.,* The upregulated intestinal folate transporters direct the uptake of ligand-modified nanoparticles for enhanced oral insulin delivery. Acta Pharm Sin B 2022,12(3):1460-72.
18.Sugumar V, Ang KP, Alshanon AF, Sethi G, Yong PV, Looi CY, *et al.,* A comprehensive review of the evolution of insulin development and its delivery method. Pharmaceutics 2022,14(7):1406.
19. Surti N, Mahajan A, Misra A. Polymers in rectal drug delivery. Aip Polym Drug Deliver 2021,263-80.
20. Karmakar S, Bhowmik M, Laha B, et al. Recent advancements on novel approaches of insulin delivery. Med Nov Technol 2023, 19: 100253.
21. Zhang T, Tang JZ, Fei X, *et al.,* Can nanoparticles and nanoprotein interactions bring a bright future for insulin delivery? Acta Pharm Sin B 2021, 11(3): 651-67.
22.houdhury RR and Mukherjee R. Polymeric nanoparticle based oral insulin delivery system. Biomed Res 2022;,33(2):30-36.
23.Benyettou F, Kaddour N, Prakasam T, *et al., In vivo* oral insulin delivery via covalent organic frameworks. Chem Sci 2021,12(17): 6037-6047.
24.Gong Y, Mohd S, Wu S, *et al.,* pH-responsive cellulose-based microspheres designed as an effective oral delivery system for insulin. ACS Omega 2021, 6(4): 2734-2741.
25. Mohanty AR, Ravikumar A and Peppas NA. Recent advances in glucose-responsive insulin delivery systems: novel hydrogels and future applications. Regen Biomater 202,; 9: rbac056.
26. Pratap-Singh A, Guo Y, Baldelli A, *et al.,* Concept for a unidirectional release mucoadhesive buccal tablet for oral delivery of antidiabetic peptide drugs such as insulin, glucagon-like peptide 1 (GLP-1), and their analogs. Pharmaceutics 2023, 15(9): 2265.
27. Olorunsola EO, Davies KG, Ibiang KP, *et al.* Prosochit®-based nanoparticulate system of insulin for oral delivery: design, formulation, and characterization. J Appl Pharm Sci 2023, 13(3): 044-052.
28. Wang T, Shen L, Zhang Y, *et al.* “Oil-soluble” reversed lipid nanoparticles for oral insulin delivery. J Nanobiotechnol 2020, 18: 98.

29. Olorunsola EO, Alozie MF, Davies KG, et al. Advances in the science and technology of insulin delivery: a review. J Appl Pharm Sci 2021, 11(8): 184-191.
30.Chellathurai MS, Yong CL, Sofian ZM, et al. Self-assembled chitosan-insulin oral nanoparticles-a critical perspective review. Int J Biol Macromol 2023, 243: 125125.
31 Adepu S and Ramakrishna S. Controlled drug delivery systems: current status and future directions. Molecules 2021,26(19): 5905.
32. Xiao Y, Tang Z, Huang X, et al. Glucose-responsive oral insulin delivery platform for one treatment a day in diabetes. Matter 2021, 4(10): 3269-3285.
33.Cheng H, Guo S, Cui Z, Zhang X, Huo Y, Guan J, et al. Design of folic acid decorated virus-mimicking nanoparticles for enhanced oral insulin delivery. Int J Pharm 2021,596:120297.